PHYSICAL REVIEW A VOLUME 23, NUMBER 1 JANUARY 1981

Extended Boltzmann analysis of electron swarm experiments

L. C. Pitchford, S. V. ONeil, and J. R. Rumble, Jr.*
Joint Institute for Laboratory Astrophysics, University of Colorado and National Bureau of Standards, Boulder, Colorado 80309
(Received 29 April 1980)

We present a method for generalizing the traditional two-term Legendre expansion solution of the Boltzmann equation in the context of electron swarm experiment analysis. The method is applied to the calculation of the distribution function and transport coefficients in N_2 and in two model cases. We find that the two-term approximation is of limited validity for the cases considered here, and that four to eight terms in the Legendre series are required for convergence of the transport coefficients to the accuracy required for the determination of cross sections from swarm experiments.

I. INTRODUCTION

Some of the most accurate values of low-energy electron scattering cross sections for atoms and molecules have been deduced from electron-swarm experiments,[1-5] studies of the motion of a cloud of electrons through a neutral gas under the influence of an electric field. The parameters measured in swarm experiments[4-9] include transport coefficients such as drift velocities and diffusion coefficients, and rate coefficients for processes such as ionization, attachment, and excitation. In these experiments the scattering is multicollisional and the determination of scattering cross sections from the experimental data is necessarily statistical. The link between the microscopic cross sections and the measured macroscopic swarm parameters is provided by the Boltzmann equation.[4,8,9] Given the cross sections for the relevant processes, one can determine the statistical behavior of an ensemble of particles and thus derive theoretical predictions for the transport coefficients. Conversely, given the measured transport parameters, one can iteratively refine a set of assumed cross sections to achieve agreement between the given parameters and those derived from the solution of the Boltzmann equation.

Experimental determination of the transport parameters can be made with high precision. Robertson[6] and Milloy and Crompton[7] for example, report, respectively, an uncertainty of 1% for the drift velocity and 2% for the diffusion measurements. The calculation of transport parameters via a Boltzmann analysis for a given set of scattering cross sections can in principle be carried out with comparable precision, although this would require a Boltzmann equation solution more accurate than has traditionally been achieved. Computational simplicity has commonly dictated a number of approximations, most notably that the velocity dependence of the electron distribution function is isotropic or nearly so, and that the angular dependence is thus adequately represented by only the first two terms of an infinite expansion in Legendre polynomials.[8,9] In terms of atomic or molecular processes, the assumption underlying the putative isotropy of the distribution function is that the cross sections for inelastic processes are much smaller than those for elastic processes.[9] This condition is well met at low energies, for example, in the rare-gas atoms, for which electronic excitation requires several electron volts and for which the usual low-energy inelastic channels in rotation and vibration are absent. For diatomics or polyatomics, however, these two channels may be available for inelastic scattering at low energies so that the conditions required for the validity of the traditional two-term expansion may not be met.

At the cost of computational complexity, one may of course retain higher terms in the Legendre expansion. The extension to three terms has been investigated by Ferrari,[10,11] Wilhelm and Winkler,[12] and more recently by Makabe and Mori.[13] As expected, the results of these workers suggest that in cases where the ratio of inelastic to elastic cross sections is large, the two-term approximation begins to break down, and it remains uncertain whether the addition of one more Legendre components is sufficient. Lin, Robson, and Mason[14] have recently presented a general moment method for calculating transport coefficients from the Boltzmann equation in which a multiterm Legendre expansion is employed. In this approach, it is the velocity moments of the distribution function rather than the function itself that are calculated.

All the methods mentioned above convert the Boltzmann partial differential equation (PDE) into a set of coupled ordinary differential equations (ODE), one such equation for each term retained in the Legendre expansion. Alternately, one might make a more direct attack, avoiding the Legendre expansion entirely and employing the techniques available for the solution of partial differential equations. This has been carried out in the work of

Kleban and Davis,[15,16] and Kitamori *et al.*[17] The drawback to this latter approach is that the state of the art for PDE's is not nearly as advanced as that for ODE's, so that while a direct solution of the Boltzmann equation as a PDE is an interesting and promising alternative, it is currently not computationally competitive.

In the Boltzmann equation, the electron ensemble in a swarm experiment is described by a probability distribution which reflects the statistical nature of the macroscopic behavior of the electrons due to a large number of individual interactions. An alternate approach, perhaps closer in spirit to the actual experiment, would be to calculate a series of electron trajectories through a gas, with the exact outcome of the collisions modeled by a random variable for each process considered.[18] Although a single such trajectory is simply evaluated, these Monte Carlo procedures are generally inefficient since they require a vast number of trajectories to achieve an accuracy comparable to that available from a Boltzmann treatment. This relative computational inefficiency is magnified to the point of infeasibility when the iterative extraction of the scattering cross sections from accurate experimental data is carried out. Such methods do, however, offer a means for verifying a solution independently derived from a given set of cross sections.

In Secs. II and III we present a new approach for the accurate solution of the Boltzmann equation describing electron swarm experiments. We employ the traditional Legendre expansion but retain as many terms as are required for convergence. The analysis is a straightforward generalization of that which leads to the two-term expansion. The resulting set of coupled ODE's is solved with a basis set Galerkin technique[19] which yields the components of the distribution function directly and which is efficient enough to allow for an iterative refinement of assumed cross sections, if necessary. Inelastic and superelastic collisions as well as anisotropic scattering are easily included in this method. For the present we ignore attachment and require that the average electron energy be low enough to preclude any appreciable change in the electron density due to ionization, although these restrictions could be lifted within our general scheme.

In Sec. IV we apply this method to two model systems and to N_2. The models chosen for investigation were methane and an ideal atom of mass 4 amu with a ramp excitation cross section. The N_2 calculations were carried out using a set of cross sections recently derived by Phelps *et al.*[20] Results of the calculations of drift velocities and transverse diffusion coefficients as functions of the number of Legendre terms are shown for these three cases.

II. TRANSPORT EQUATIONS

The dynamics of an ensemble of electrons drawn through a neutral gas by an external electric field is much too complicated to admit any consideration of the detailed results of the repeated scattering events involved, although the result of an individual event is described by the relevant scattering cross sections. Rather, the scattering processes are described statistically by considering particles of the neutral gas to be interacting with electrons described by a time-dependent probability distribution $F(\vec{r},\vec{v},t)$, given in terms of the position and velocity coordinates of the electron. The electron number density $n(\vec{r},t)$ is given by the integral of $F(\vec{r},\vec{v},t)$ over all velocities, $n(\vec{r},t) = \int F(\vec{r},\vec{v},t)d\vec{v}$.

If we restrict our interest to cases for which there is no ionization or attachment, the total number of electrons is conserved, although electron density may flow from one region of phase space to another through the action of the external field and the interactions with the buffer gas. The precise description of how the density flows is given by the familiar Boltzmann equation[8]:

$$\frac{\partial}{\partial t}F(\vec{r},\vec{v},t)+\vec{a}\cdot\vec{\nabla}_v F(\vec{r},\vec{v},t)+\vec{v}\cdot\vec{\nabla}_r F(\vec{r},\vec{v},t) = J[F(\vec{r},\vec{v},t)], \quad (1)$$

which gives the evolution of F in terms of its space and velocity gradients, the acceleration produced by the applied field ($\vec{a}=-e\vec{E}/m$), and the collisions with the gas as represented by the right-hand side.

Transient effects and the detailed nature of the early-time evolution of the swarm are of little interest in most swarm experiments, so the distribution function can be taken to obey the so-called "hydrodynamic conditions." A detailed discussion of these conditons is unnecessary here, but the appropriate picture is that of a swarm evolving without memory of initial conditions or influence of boundary constraints. Making use of this "smoothness" and in preparation for the subsequent separation of position (and time) and velocity variables, we follow the procedure of Skullerud[21,22] by expanding the distribution function in a series in powers of the spatial gradient of the number density:

$$F(\vec{r},\vec{v},t)=\sum_{k=0}^{\infty}\underline{f}^{(k)}(\vec{v})\otimes(-\vec{\nabla})^k n(\vec{r},t), \quad (2)$$

where $(\vec{\nabla})^k$ represents a k-fold outer product of the gradient operator with itself and $\otimes$ indicates a k-fold inner-product operation. The coefficients in the expansion, $\underline{f}^{(k)}(\vec{v})$, are velocity-dependent tensors of rank k. When coupled with the appropriate power of $\vec{\nabla}n(\vec{r},t)$, $\underline{f}^{(k)}$ yields the kth-order correc-

tion to the simple situation in which $F(\vec{r},\vec{v},t)$ is a separable product of velocity and density distributions.

The hydrodynamic regime admits an alternate but related description[21] based solely on the number density and a hierarchy of tensorial transport coefficients, $\underline{\omega}^{(k)}$. In this description the evolution of the number density is given as

$$\frac{d}{dt}n(\vec{r},t)=\sum_{k=0}^{\infty}\underline{\omega}^{(k)}\otimes(-\vec{\nabla})^{k}n(\vec{r},t)\,. \tag{3}$$

For a uniform electron density [$(\vec{\nabla})^{k}n=0$, for all $k>0$], this reduces to the familiar first-order kinetic rate equation, with $-\omega^{(0)}$ identified with the reaction rate. The higher-order effects of a nonuniform density are included with the drift velocity $\vec{\omega}^{(1)}=\vec{W}$, the diffusion tensor $\underline{\omega}^{(2)}=\underline{D}$ (the diagonal components of which relate to measured quantities), and the remaining members of the hierarchy. The first few transport coefficients are the parameters measured in a swarm experiment, and they thus provide the link between the theoretical description of the dynamics of a swarm and some of its experimentally determined properties.

The hierarchy of transport coefficients can be determined by developing a corresponding hierarchy of kinetic equations. Following the standard procedure,[21] we substitute the form of F given by Eq. (2) into the Boltzmann equation, (1), and after interchanging the order of differentiation, simplify the result by using Eq. (3). Noting the linear independence of the various $(\vec{\nabla})^{k}n(\vec{r},t)$ by virtue of their differing rank, we arrive at the desired hierarchy

$$\vec{a}\cdot\vec{\nabla}_{v}f^{(0)}(\vec{v})-J[f^{(0)}(\vec{v})]+\omega^{(0)}f^{(0)}(\vec{v})=0\,, \tag{4a}$$

$$\vec{a}\cdot\vec{\nabla}_{v}\underline{f}^{(k)}(\vec{v})-J[\underline{f}^{(k)}(\vec{v})]=\vec{v}\,\underline{f}^{k-1}(\vec{v})-\sum_{j=0}^{k}\underline{\omega}^{(j)}\underline{f}^{(k-j)}(\vec{v})\,. \tag{4b}$$

For the conditions we mentioned previously, in which no attachment or ionization is allowed to increase or decrease the total number of electrons, the reaction rate $\omega^{(0)}$ is identically zero and the only effect of the collision operator is to redistribute the density in phase space. With a unit normalization of the distribution function, we see that integration of Eq. (4b) over velocity then gives $\underline{\omega}^{(k)}$ directly in terms of $\underline{f}^{(k-1)}(\vec{v})$:

$$\underline{\omega}^{(k)}=\int\vec{v}\underline{f}^{(k-1)}(\vec{v})d\vec{v}\,.$$

Knowledge of terms up to $\underline{f}^{(k)}$ and $\underline{\omega}^{(k)}$ thus provides all the information required to determine $\underline{\omega}^{(k+1)}$ and hence $\underline{f}^{(k+1)}$.

Since $\omega^{(0)}$ vanishes, $f^{(0)}$ can be determined from Eq. (4a) alone. Rather than solving this partial differential equation as it stands, we follow the usual procedure and expand the vector dependence of the scalar function $f^{(0)}$ as a Legendre series in the angular coordinates of the velocity

$$f^{(0)}(\vec{v})=\sum_{l}f_{l}^{(0)}(v)\,P_{l}(\cos\theta)\,. \tag{5}$$

Substituting this into Eq. (4a) and employing the orthogonality of the P_l's, we obtain an infinite set of tridiagonally coupled ordinary differential equations in the scalar variable $v=|\vec{v}|$. In practice this infinite set is truncated at some finite $l=L$, with L chosen large enough to ensure "convergence" of the expansion in Eq. (5), as discussed in Sec. IV. Similar equations result from Eq. (4b) for $\vec{f}^{(1)}$. In what follows, we discuss $f^{(0)}(\vec{v})$, and, dropping the superscript for simplicity, let $f^{(0)}(\vec{v})\equiv f(\vec{v})$. It is understood that the same discussion applies to each component of the tensor $\underline{f}^{(k)}(\vec{v})$ for all k.

The form of the collision operator J has been described in detail by Holstein,[9] Allis,[8] and others[4,22] and may be written as

$$J[f(\vec{v})]=-NvQ(v)f(\vec{v})+\frac{N}{v^{2}}\sum_{k=0}\int v'f(\vec{v}')Q_{k}(v',\theta_{s})\,\delta(v'-g(v))d\vec{v}'\,. \tag{6}$$

Here N is the neutral number density and $Q_k(v,\theta_s)$ is the cross section for electrons incident at velocity v and scattered by a particular process (the kth such process considered) with a scattering angle θ_s. $Q(v)$ is the sum of all the individual cross sections evaluated at an identical argument and integrated over all angles. The first term on the right side of Eq. (6) thus represents the depletion of density from the region of $\vec{v}$ due to all scattering processes. The second term is then the accretion of density into the region of $\vec{v}$ from all other regions of velocity $\vec{v}'$ and the sum is over all possible channels, with $k=0$ denoting the elastic one. The presence of the Dirac delta functions simply reminds us that if the kth scattering process is to take place, then the final energy of the electron must be consistent with whatever energy was required for (or released by) the alteration of internal states of the neutral particle mediating that process.

At this point we display explicitly in energy space the infinite set of tridiagonally coupled ordinary differential equations resulting from substituting the Legendre expansion (5) and the collision operator (6) into Eq. (4a):

$$\frac{l}{2l-1}\left(\epsilon\frac{df_{l-1}(\epsilon)}{d\epsilon}-\frac{l-1}{2}f_{l-1}(\epsilon)\right)+\frac{l+1}{2l+3}\left(\epsilon\frac{df_{l+1}(\epsilon)}{d\epsilon}+\frac{l+2}{2}f_{l+1}(\epsilon)\right)$$
$$=\frac{N}{E}\epsilon Q(\epsilon)f_l(\epsilon)-\frac{N}{E}\epsilon f_l(\epsilon)\int P_l(\cos\theta_s)Q_0(\epsilon,\theta_s)d\omega'+2\frac{m}{M}\frac{N}{E}\frac{d}{d\epsilon}[\epsilon^2Q_m f_l(\epsilon)]\,\delta_{l0}$$
$$-\frac{N}{E}\sum_{k=1}(\epsilon+\epsilon_k)f_l(\epsilon+\epsilon_k)\int P_l(\cos\theta_s)Q_k(\epsilon+\epsilon_k,\theta_s)d\omega',\quad \text{for } l=0,\ldots,L. \tag{7}$$

Q_m is the momentum transfer cross section for elastic scattering, i.e., the integrated elastic cross section weighted by the factor $(1-\cos\theta)$, and ϵ_k is the threshold energy for the kth process. The details of the rearrangement of the collision terms are given by Holstein.[9] The next-to-last term on the right is the recoil energy loss. The only contribution from elastic scattering in the $l=0$ equation arises from this recoil term. The recoil term also contributes to the $l>0$ equations, but, as indicated by the Kronecker delta function, it is neglected because its contribution to the total collision term will be small. In going from Eq. (4a) to Eqs. (7), a partial differential equation has been converted to $L+1$ ordinary differential equations. The principal merit to this step comes from the fact that an accurate solution can be found with L relatively small.

Besides retaining more Legendre components, Eqs. (7) offer the additional generality over the usual two-term equations that anisotropic scattering is included up to order P_L in the cross sections. In addition, the inclusion of superelastic processes in Eqs. (7) can be done in a natural and straightforward manner,[5] replacing N in the last term of Eqs. (7) by the populations of the appropriate excited states and the positive energy offset $(\epsilon+\epsilon_k)$ by a negative offset $(\epsilon-\epsilon_k)$. The total cross section must then include the superelastic contributions.

III. SOLUTION OF THE TRANSPORT EQUATIONS

The development reviewed in Sec. II casts the Boltzmann equation for an electron swarm into the form of a coupled system of linear ordinary differential equations in the scalar variable v:

$$\mathfrak{A}\vec{f}=\vec{r}, \tag{8}$$

where $\vec{r}$ can be identified with the right-hand sides of Eq. (4). The components of the vector $\vec{f}$ are the Legendre expansion coefficients $f_l(v)$. The elements of the matrix $\mathfrak{A}$ are the differential, multiplicative, and integral operators displayed explicitly in Eqs. (7). $\mathfrak{A}$ is a nonlocal operator if it retains terms in Eqs. (7) which represent nonelastic collisions, i.e., terms in which the argument of f_l is $\epsilon\pm\epsilon_k$.

The backward prolongation method of Sherman[23] has been utilized extensively in solving Eq. (8) for the nearly isotropic case ($L=1$). Following Sherman,[23] Frost and Phelps,[5] for example, assumed that in the high-energy regime the solution of (8) matched the solution for purely elastic scattering and used these initial conditions with a direct numerical integration of (8) to propagate the solution to lower energies. If superelastic processes are important, this procedure is inapplicable since the information required to calculate f at any given ϵ includes knowledge of $f(\epsilon-\epsilon_k)$, a quantity which is not available until later (smaller ϵ) in the integration. Similar difficulties result if the solution is started at $\epsilon=0$.

An alternate approach[17] replaces the differential terms in (8) with their finite-difference approximations at a number of grid points. The resulting linear algebraic system is then solved for the value of the function f at the grid points. This algorithm is easy to implement and circumvents the difficulties arising from the nonelastic terms, but convergence as a function of the grid spacing h is typically proportional to only h^2, so that a highly accurate solution requires very small h, and thus very large algebraic systems.

The Galerkin method retains the generality and ease of implementation characteristic of a finite-difference approach, but possesses much more desirable convergence characteristics. It has been well presented elsewhere,[19] but in order to fix ideas, we review how it applies for the simple case where (8) is a single integro-differential equation. Galerkin's method calls for the expansion of the unknown function in terms of a finite but flexible set of basis functions $[S_j]$:

$$f(\epsilon)=\sum_{j=1}^{N}C_jS_j(\epsilon)+\delta(\epsilon), \tag{9}$$

with the S's known functions, the C_j's as yet undetermined, and $\delta(\epsilon)$ a small error term. Equation (8) now becomes

$$\sum_{j=1}^{N}C_j\mathfrak{A}S_j(\epsilon)-r(\epsilon)=\delta(\epsilon). \tag{10}$$

For any finite set of basis functions the error term in (10) will be nonzero. The error can, however, be forced to have zero projection in the linear space spanned by the basis by requiring that

$$\langle S_i(\epsilon)|\mathfrak{G}|\delta(\epsilon)\rangle = 0\,, \quad \text{for } i=1,N\,, \tag{11}$$

where for any two functions h and g the inner product is

$$\langle h|g\rangle = \int_0^\infty h(\epsilon)\,g(\epsilon)d\epsilon\,.$$

Substitution of (10) into (11) gives a set of N linear algebraic equations in the N unknown coefficients C_j:

$$\sum_j C_j\langle S_i(\epsilon)|\mathfrak{G}|S_j(\epsilon)\rangle - \langle S_i(\epsilon)|r\rangle = 0\,, i=1,2,\ldots N \tag{12}$$

or in matrix form with obvious notation

$$\underline{B}\vec{C} - \vec{R} = 0\,. \tag{13}$$

The boundary conditions which augment (13) to completely specify the solution to the system (8) follow from the normalization

$$\int f(\vec{v})d\vec{v} = 1\,. \tag{14}$$

In light of Eq. (5), the orthogonality of the P_l's, and after converting to energy space, the normalization conditions become

$$\int_0^\infty \epsilon^{1/2}f_0(\epsilon)d\epsilon = \frac{1}{2\pi}\left(\frac{2e}{m}\right)^{-3/2}, \tag{15a}$$

$$\int_0^\infty \epsilon^{1/2}f_l(\epsilon)d\epsilon < \infty\,, \quad \text{for } l>0\,. \tag{15b}$$

Provided that each member of the basis is integrable, the mild conditions of (15b) are ensured if each component of $\vec{C}$ is finite. The normalization (15a) can be enforced explicitly.

There are several advantages of this method. The original set of coupled integro-differential equations is converted to a system of linear algebraic equations which can be solved accurately and highly efficiently, especially on modern vector processing computers. The nonlocal nature of $\mathfrak{G}$ is simply and directly accounted for in evaluating the projection integrals in Eq. (12), and does not appear explicitly in Eq. (13). For special choices of basis functions, the elements of the matrix B can be easily and accurately evaluated analytically, while for more general bases the elements can be evaluated numerically by appropriate quadrature techniques. Finally, the extension to coupled systems, such as those treated in Sec. IV, is straightforward.

The primary criteria in selecting a particular basis $[S_i]$ are flexibility and ease of manipulation. By a flexible basis we mean one that not only represents all members of a coupled set equally well but also which represents the solutions equally well in all energy regions of interest. An easily manipulated basis is important if the integrals appearing in (12) are to be evaluated efficiently. A basis which well satisfies both these criteria is provided by a set of cubic B-splines.[24] These are piecewise continuous cubic polynomials defined on a partition $(\epsilon_0=0,\ \epsilon_1,\ldots,\ \epsilon_n=\epsilon_{max})$. The value of $S_i(\epsilon)$ is zero

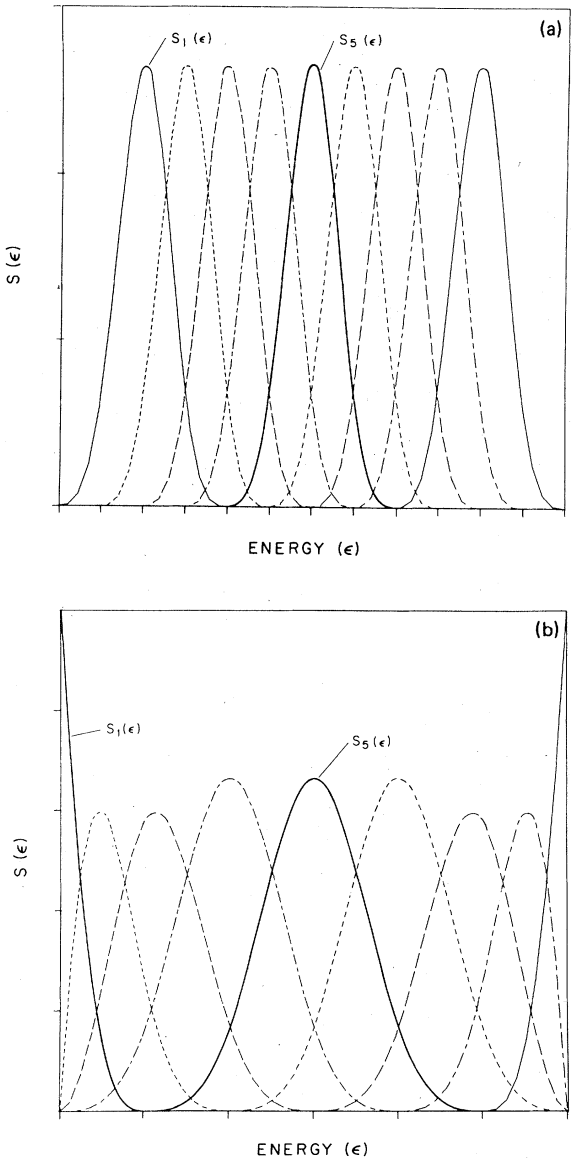

FIG. 1. (a) An expansion basis consisting of 9 cubic B-splines defined on an equally spaced grid, with the basis function S_5 accentuated. The basis shown can be used for the approximate expansion of a smooth function which vanishes at zero and ϵ_{max}. (b) An expansion basis set consisting of 9 cubic B-splines defined on a grid which is nonuniform near the endpoints. The basis shown can be used for the approximate expansion of a smooth function which is finite at the points zero and ϵ_{max}. For the expansions discussed in this work, the range $[0, \epsilon_{max}]$ was spanned by up to 100 such basis functions.

outside the range $[\epsilon_i, \epsilon_{i+4}]$, and within that range S_i is greater than zero and has a single maximum. For a uniform partition, with $\epsilon_{i+1} - \epsilon_i = h$ for all i, the basis is composed of individual B-splines replicated along the energy axis, as shown in Fig. 1. In practice it is more efficient to adjust the partition so that the grid points ϵ_i (and therefore the spline basis functions) are more closely spaced in energy regions where the solution is expected to vary rapidly or display fine structure. For the calculations discussed in the next section, the spacing $(\epsilon_{i+1} - \epsilon_i)$ was proportional to $\epsilon_i^{1/2}$.

For this basis all the integrals required for our model problems can be evaluated analytically by taking advantage of the piecewise polynomial nature of B-splines. But in applications to experimental systems, for which the electron-neutral cross sections are not usually available in simple analytical form, some of the integrals would require numerical quadrature. We therefore chose to evaluate all the integrals numerically using range-splitting, with a Gauss-Legendre quadrature rule applied in each grid range $[\epsilon_i, \epsilon_{i+1}]$.

The solution of the coupled differential system (8) will depend on the boundary conditions and the physical parameters appearing in (7), i.e., the positions of thresholds, the cross sections, etc. The solution of the Galerkin projected equations (12) will in addition, depend on the mathematical parameters which specify the basis $[S_i]$. For the Galerkin solution to be reliable, we must insist that, within some prescribed tolerance, it is independent of the nonphysical parameters, although its mathematical form will usually retain some dependence. In the case of our B-splines basis, we require that the computed solution be independent of the number of splines, the precise position of the grid points ϵ_i, and the energy limit $\epsilon_{\max}$. In practice this is achieved by increasing the number of splines and the value of $\epsilon_{\max}$ until the numerical value of $f_1(\epsilon)$ in the energy range of interest stabilizes to several significant figures. Although the number of basis splines necessary to achieve such convergence depends on the cross-section data, we find that 100 splines is sufficient in the worst cases.

One drawback to the choice of a B-spline basis is the large number of basis functions needed, and hence the size of the coefficient matrix $\underline{B}$ which must be stored. Although some economy results from the block tridiagonal form of $\underline{B}$, it is true that the advantages of this basis are best realized on modern large-scale vector processors. In this environment, the disadvantage of storing a large B matrix is more than offset by the speed with which the linear system (8) can be formed and solved. A typical calculation for the methane model, using a basis of 120 B-splines and retaining Legendre terms through $L = 3$, required about 3 sec of Cray-1 time to form the linear system (13) and $\frac{1}{3}$ sec to obtain the solution vector. Direct comparison of this efficiency with that of alternate methods is difficult because our approach was intended to take advantage of the vector processing capabilities of a particular computer.

IV. NUMERICAL RESULTS

Many of the properties of the calculated distribution function, in particular the convergence properties, can be seen in simple model cases. In this section we discuss the numerical solutions for a model atom and a methane model, each with a single inelastic cross section. We then examine the results for N_2, using a set of cross sections determined from a two-term Boltzmann analysis of swarm data. In all three cases the scattering is assumed isotropic, and superelastic collisions are neglected. The transport coefficients discussed in this section are the drift velocity, $W = |\vec{W}|$, and the characteristic energy, D_T/μ. The electron mobility, μ, is W/E, and the transverse diffusion coefficient is $D_T = \omega_{xx}^{(2)} = \omega_{yy}^{(2)}$. The parameters W, D_T/μ, and the average electron energy are functions of E/N, the ratio of the electric-field strength to the neutral number density.[4]

A. Model atom

The simplest system we have examined is the model atom of Reid. His Monte Carlo results[25] are available for comparison with our own, and the model allowed a thorough convergence study. The elastic cross section for this model is constant at 6×10^{-16} cm^2 and the inelastic cross section is of the form $(\epsilon - 0.2) \times 10^{-15}$ cm^2, i.e., a ramp with a threshold energy at 0.2 eV. The neutral mass is 4 amu. The E/N values considered range from 1×10^{-17} to 24×10^{-17} V cm^2, yielding corresponding distribution functions with average energies ranging from well below the inelastic threshold to well above.

Since calculated values of transport coefficients are directly comparable to the corresponding experimental quantities, it is these quantities on which we focus. In particular, we would like to examine how these quantities are affected by truncating the Legendre expansion for the distribution function at $L = 1$, as is usually done. We have calculated values of W and D_T/μ, using as many terms as are required to converge W to 0.1% and D_T/μ to 1%. Table I shows the calculated transport coefficients as a function of L for the model atom at three values of E/N. The two-term values of W and D_T/μ are always greater than the converged

TABLE I. Model atom.

E/N (10^{-17} V cm^2)	L	W (10^6 cm sec^{-1})	D_TN (10^{22} cm^{-1} sec^{-1})	D_T/μ eV
1	1	1.275	0.9905	0.0777
1	3	1.272	0.9746	0.0766
1	5	1.272	0.9750	0.0766
1	7	1.272	0.9749	0.0766
1	MC	1.255 ± 0.013	0.9861 ± 0.020	0.0786
12	1	7.029	1.369	0.234
12	3	6.841	1.110	0.195
12	5	6.838	1.134	0.199
12	7	6.839	1.134	0.199
12	MC	6.87 ± 0.069	1.168 ± 0.023	0.204
24	1	9.143	1.438	0.377
24	3	8.887	1.095	0.296
24	5	8.885	1.132	0.306
24	7	8.883	1.130	0.305
24	MC	8.890 ± 0.089	1.194 ± 0.024	0.322

values, and D_T/μ is more sensitive than W to the two-term truncation. The values of W and D_T/μ appear to converge quite rapidly with increasing L. As expected, the largest changes occur between $L = 1$ and $L = 3$, with much smaller changes from further increases in L.

The rows labeled "MC" in Table I are results of a Monte Carlo calculation.[25] The uncertainty indicated in the table reflects the estimated accuracy of the Monte Carlo calculations; 1% for W and 2% for D_T/μ. Our converged results compare well with the Monte Carlo values, providing an independent check on our numerical methods.

A more sensitive test of convergence is furnished by examining the individual Legendre expansion coefficients f_l. Figure 2 displays the f_l for $l = 0$ to 5 at an E/N of 24×10^{-17} V cm^2. At this field strength the two-term approximation is clearly inadequate. The zero in each of the higher-order coefficients occurs at successively higher energies, and the extrema in each f_l ($l \geq 2$) are separated by approximately the same energy. On the high-energy side of the zeros all of the f_l's decay at approximately the same rate. It can also be seen that successively higher-order components dominate as the energy increases, due to the increasing ratio of inelastic to elastic cross sections.

Figure 3 shows the convergence of f_0 and f_1 as L is increased from 1 to 5. The two-term results ($L = 1$) underestimate the converged values at both low and high energy and overestimate them at the intermediate energies. This pattern is reflected in the values of the integrals determining W and D_T/μ, for which the intermediate-energy region contributes most heavily. Thus, the converged values of these transport coefficients are correspondingly less than the two-term results.

B. Methane

Methane is particularly interesting because of the large value of the inelastic cross section in the region of the Ramsauer minimum in the elastic

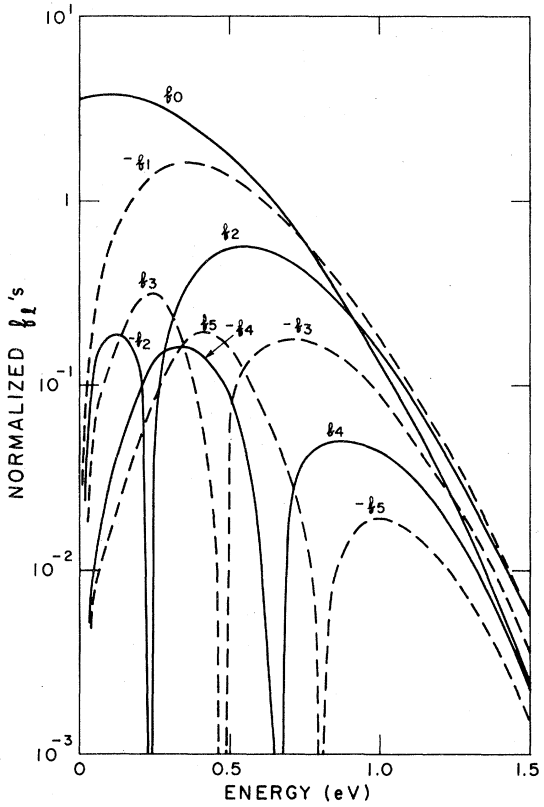

FIG. 2. The first six Legendre expansion coefficients, f_l for $l = 0$ to 5, as a function of energy for the model atom with $E/N = 24 \times 10^{-17}$ V cm^2.

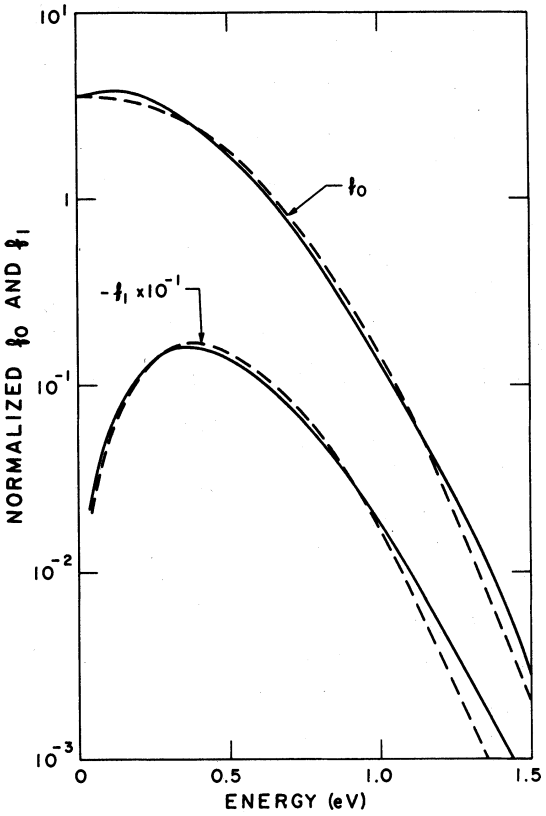

FIG. 3. Comparison of f_0 and f_1 from the two-term (dashed lines) and six-term (solid lines) solutions for the model atom with $E/N = 24 \times 10^{-17}$ V cm^2.

cross section. The previously noted criterion for the validity of the two-term approximation, i.e., a small ratio of inealstic to elastic cross sections, thus fails in this case and we may anticipate a corresponding inaccuracy in the two-term results themselves.

For our model methane calculations we adopted the cross sections of Kleban and Davis,[15,16] and introduced a modification below 0.169 eV to avoid the singular behavior in their zero-energy elastic cross section. These cross sections are somewhat crude, but do qualitatively reproduce the general features of the transport data. The cross sections are presented in Fig. 4.

Figure 5 shows results of calculations of W and D_T/μ for $L = 1$ and 5 over a range of E/N around the maximum in W. As E/N increases, the converged ($L = 5$) results and the two-term approximate results differ by as much as 34% for D_T/μ and 6.4% for W. The point of maximum error corresponds roughly to the E/N where the average energy of the swarm passes into the region of the Ramsauer minimum. At that point, most of the collisions the electrons suffer are inelastic. The six-term values of the expansion coefficients f_l are shown in Fig. 6 for $E/N = 2.42 \times 10^{-17}$ V cm^2. The main features seen in the case of the model atom can also be seen here, in particular the zeros and two extrema in the higher-order coefficients. Figure 7 shows f_0 and f_1 for $L = 1$ and 5. The two-term solution again tends to overestimate f_0 and f_1

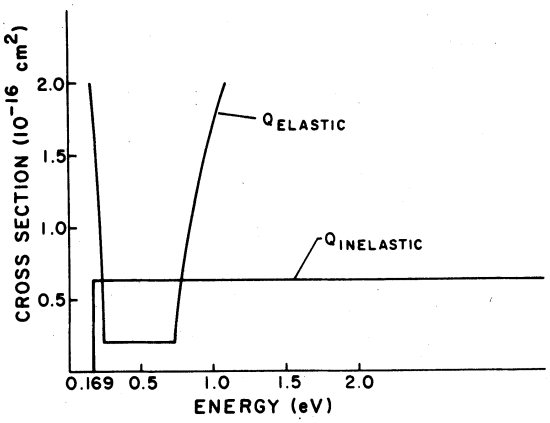

FIG. 4. Model methane cross sections used in the calculations here. The elastic cross section $Q_0(\epsilon)$ is equal to the following: 2.14×10^{-16} cm^2, $\epsilon < 0.169$ eV; $(0.654/\epsilon - 2.36) \times 10^{-16}$ cm^2, $0.169 < \epsilon < 0.256$ eV; 0.2×10^{-16} cm^2, $0.256 < \epsilon < 0.712$ eV; $(9.88\epsilon^{1/2} - 8.133) \times 10^{-16}$ cm^2, $\epsilon > 0.712$ eV. The inelastic cross section rises at threshold in a step from zero to a constant for $Q_k(\epsilon)$ equal to the following: 0, $\epsilon \leq 0.169$ eV; 0.63×10^{-16} cm^2, $\epsilon > 0.169$ eV.

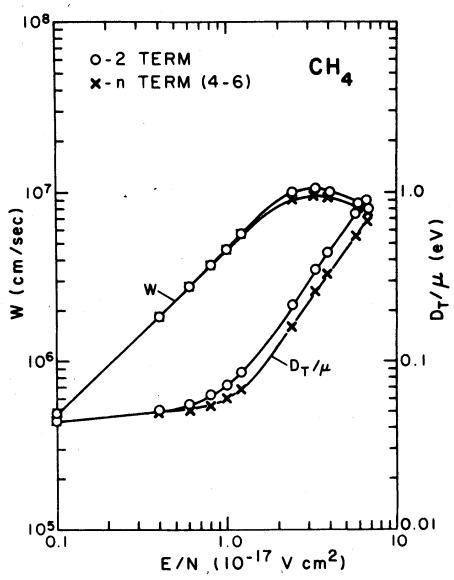

FIG. 5. The transport coefficients W and D_T/μ as a a function of E/N calculated for $L = 1$ (two terms) and $L = 5$ (six terms) in methane at 2.42×10^{-17} V cm^2.

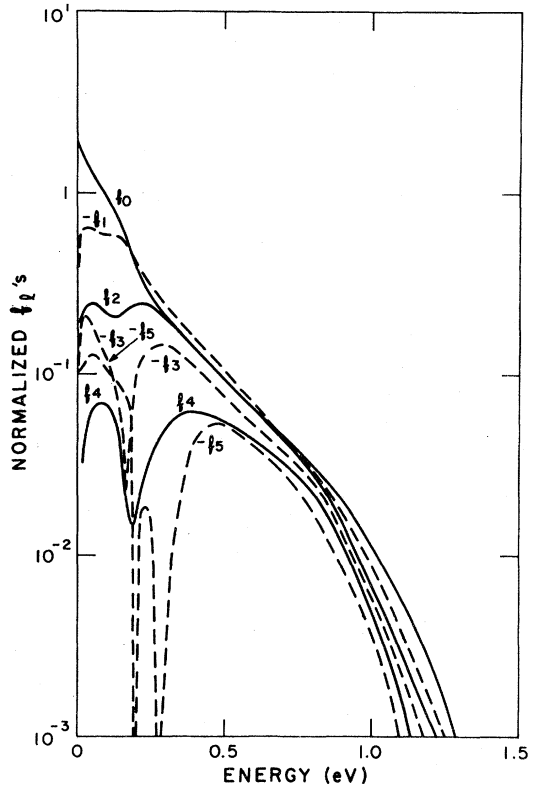

FIG. 6. The first six Legendre expansion coefficients, f_l for $l = 0$ to 5, as a function of energy for methane at 2.42×10^{-17} V cm^2.

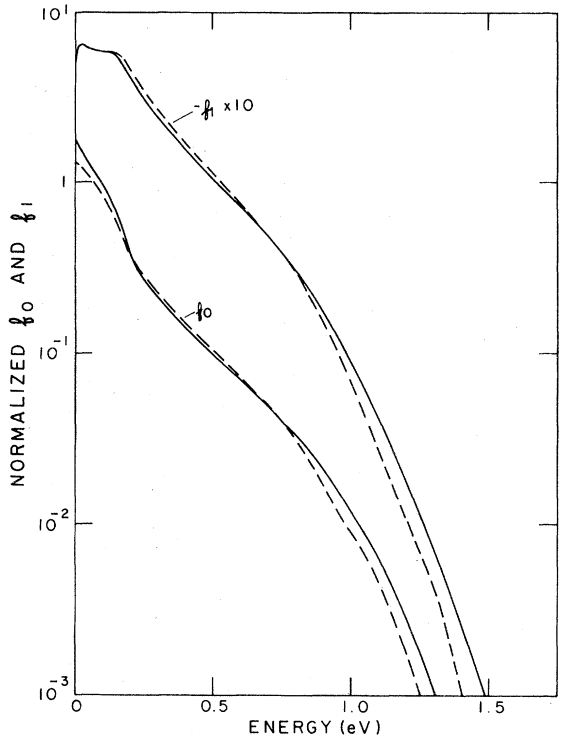

FIG. 7. Comparison of f_0 and f_1 from the two-term (dashed lines) and six-term (solid lines) solutions in CH_4 at 2.42×10^{-17} V cm^2.

for the intermediate energies and underestimates their values at higher energies. These results demonstrate that the two-term approximation is inaccurate for CH_4 at this range of E/N, although the error seems to be decreasing slightly as E/N is increased beyond 3.9×10^{-17} V cm^2.

C. Nitrogen

As a final study, we have used our general electron swarm Boltzmann method to examine transport in N_2. Our aim is to apply the method developed above to a case in which many inelastic channels are open. The cross sections used were those derived by Phelps *et al.*,[20] and include eight vibrational and twelve electronic excitation processes.

Tables II and III shows the results for W and D_T/μ as a function of L for $L = 1$, 3, and 5 for six values of E/N. The calculated transport parameters have converged as a function of L to 0.1% for W and 1.8% for D_T/μ. It is expected on the basis of the results seen in Table III that the convergence of D_T/μ could be improved with the addition of a few more terms. We note again that in N_2, as in the two model cases, most of the error in the two-term approximation is removed by extending the calculation to four terms, but for very precise cal-

TABLE II. N_2 drift velocity (W).

E/N (10^{-17} V cm^2)	$L = 1$ (10^6 cm sec^{-1})	$L = 3$ (10^6 cm sec^{-1})	$L = 5$ (10^6 cm sec^{-1})
1	0.4118	0.4118	0.4118
40	5.636	5.559	5.558
70	8.589	8.439	8.434
83.3	9.735	9.580	9.572
100	11.11	10.96	10.95
200	18.67	18.54	18.53

TABLE III. N_2 diffusion coefficient/mobility (D_T/μ).

E/N (10^{-17} V cm^2)	$L=1$ (eV)	$L=3$ (eV)	$L=5$ (eV)
1	0.3213	0.3203	0.3203
40	1.239	1.161	1.174
70	1.461	1.340	1.348
83.3	1.624	1.488	1.515
100	1.888	1.739	1.773
200	3.698	3.379	3.426

culations six terms are necessary for all except the lowest values of E/N.

The error in the two-term values of W and D_T/μ does not seem to increase with increasing E/N past about 7.0×10^{-16} V cm^2, but rather levels off and even declines slightly. It is interesting to note, however, that the difference between the four-term and six-term values of W and D_T/μ also reaches a peak at an E/N near where the average energy of the swarm "sees" the largest total inelastic cross section. Based on our results in methane, we might expect the slowest convergence of the Legendre series in this region.

Figure 8 is a plot of the two-term and six-term values f_0 as a function of energy in N_2 at 1×10^{-15} V cm^2. The high-energy tail is significantly higher for the six-term calculation. Any integrals over the tail, such as those entering the calculation of excitation rates, will be correspondingly greater.

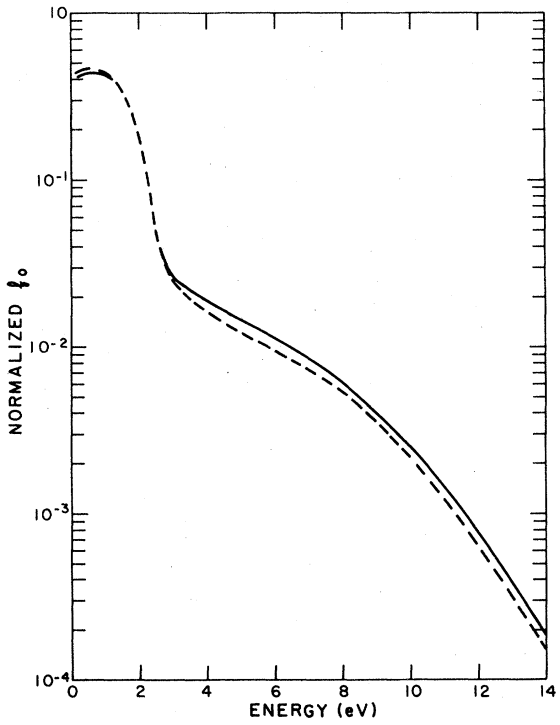

FIG. 8. Comparison of f_0 from the two-term (dashed lines) and six-term (solid lines) solutions in N_2 at 1×10^{-15} V cm^2.

V. CONCLUSIONS

The determination of low-energy electron scattering cross sections from swarm experiments has previously relied almost exclusively on the two-term Legendre expansion of the Boltzmann distribution function. We have presented a generalization that retains an arbitrary number of terms, and have applied it to the calculation of the distribution function and transport coefficients in two model cases and in nitrogen. For each of the cases we considered, we found the two-term approximation to be of limited validity, incurring errors in D_T/μ, for example, which varied from less than 1% in the best case to 35% in the worst. For methane the error is large enough to cast considerable doubt on cross sections derived from methane swarm experiments via an analysis based on the two-term approximation.

As a function of electron energy, the error in the distribution function introduced by the two-term approximation is a complicated function of the cross sections. We find that the distribution function is most slowly convergent for electron energies at which the ratio of the inelastic to elastic cross section is maximum. For CH_4 this occurs in the region of the Ramsauer minimum and for N_2 around 2.0 eV where the total vibrational excitation cross section peaks. For our model atom with its inelastic cross section linearly increasing, the maximum discrepancy occurs in the high-energy tail of the distribution function.

As a function of E/N, the deviations between our converged transport coefficients and those calculated with the two-term approximation correlate well with the above observations. The error is greatest at values of E/N which produce mean electron energies close to the values where the inelastic to elastic cross-section ratio is greatest. Thus, in CH_4 the error in the transport coefficients reaches a maximum at values of E/N for which the mean energy of the electron swarm is near the region of the Ramsauer minimum. Similarly, the error in the N_2 transport coefficients begins to fall slightly for E/N large enough to produce a mean electron energy beyond the peak in the total inelastic cross section.

Convergence to within 0.1% for W was achieved for all cases considered with six or fewer terms in the Legendre expansion for the energy distribution function. While the convergence of D_T/μ was

slower, six terms were sufficient to converge our calculated values to 1% or less in the two model cases and to less than 2% for all values of E/N in N_2. We conclude from this that the Legendre series is indeed appropriate for the solution of the Boltzmann equation in the present context, as the series approximating the distribution function converges sufficiently rapidly to make accurate multiterm solutions practical.

Kumar, Robson, and Skullerud[22] have recently suggested that theoretical calculations of W and $D_T N$ should ideally be accurate to within 0.1% and 1%, respectively, in light of the extremely accurate experimental measurements with which they must be compared. Our results indicate that while the two-term approximation cannot generally deliver such accuracy, the generalization to six or eight terms can be expected to reliably and efficiently yield transport coefficients which fall within the suggested error bounds.

ACKNOWLEDGMENTS

We would like to thank W. P. Allis, E. C. Beaty, and especially A. V. Phelps for many discussions and helpful comments. We would also like to acknowledge a generous grant of computer time from the National Center for Atmospheric Research, administered by the National Science Foundation. This work was supported in part by Wright-Patterson Air Force Base under Contract No. FY1455 7900609, and in part by the National Science Foundation under Grant No. PHY79-04928.

---

*Present address: Office of Standard Reference Data, National Bureau of Standards, Washington, D.C. 20234.

[1]H. B. Milloy and R. W. Crompton, Phys. Rev. A 15, 1847 (1977).

[2]P. Mitchell and R. Winkler, Beit. Plasmaphys. 16, 233 (1976).

[3]H. T. Saelee and J. Lucas, J. Phys. D 10, 343 (1977).

[4]L. E. H. Huxley and R. W. Crompton, *The Diffusion and Drift of Electrons in Gases* (Wiley, New York, 1974). For a summary of cross sections determined from swarm experiments to 1973, see Chap. 13.

[5]L. S. Frost and A. V. Phelps, Phys. Rev. 127, 1621 (1962).

[6]A. E. Robertson, Aust. J. Phys. 30, 39 (1977).

[7]H. B. Milloy and R. W. Crompton, Aust. J. Phys. 30, 51 (1977).

[8]W. P. Allis, in *Handbuch der Physik*, edited by S. Flügge (Springer, Berlin, 1956), Vol. 21, pp. 383–444.

[9]T. Holstein, Phys. Rev. 70, 367 (1946).

[10]L. Ferrari, Physica (Utrecht) 81A, 276 (1975).

[11]L. Ferrari, Physica (Utrecht) 85C, 161 (1977).

[12]J. Wilhelm and R. Winkler, Ann. Phys. (Leipzig) 23, 28 (1969).

[13]T. Makabe and T. Mori, J. Phys. (Paris) Colloq. 40, 43 (1979).

[14]S. L. Lin, R. E. Robson, and E. A. Mason, J. Chem. Phys. 71, 3483 (1979).

[15]P. Kleban and H. T. Davis, Phys. Rev. Lett. 39, 456 (1977).

[16]P. Kleban and H. T. Davis, J. Chem. Phys. 68, 2999 (1978).

[17]K. Kitamori, H. Tagashira, and Y. Sakai, J. Phys. D 11, 283 (1978). Although this reference discusses a finite-difference approach of solving Eq. (4a) using a two-dimensional grid, the simplification of the method for solving Eq. (8) with a one-dimensional grid is obvious and the comments apply to both cases.

[18]A. I. McIntosh, Aust. J. Phys. 27, 59 (1974).

[19]A lucid pedagogical account of Galerkin's method is given by N. L. Schryer in Bell Laboratories Computing Science Technical Report No. 52, 1976 (unpublished). Schryer's bibliography also lists a number of articles which discuss Galerkin's method on a more technical level.

[20]A. V. Phelps, D. Levron, and K. Tachibana, in *Proceedings of the XIth International Conference on the Physics of Electronic and Atomic Collisions*, edited by K. Takayanagi and N. Oda (The Society for Atomic Collision Research, Kyoto, 1979).

[21]H. R. Skullerud, J. Phys. B 2, 696 (1969).

[22]K. Kumar, H. R. Skullerud, and R. E. Robson, (to be published in Aust. J. Phys.).

[23]B. Sherman, J. Math. Anal. Appl. 1, 342 (1960).

[24]The properties of B splines are presented by P. Prenter, *Splines and the Variational Method* (New York, Wiley, 1975). For efficient and general algorithms for the evaluation of B splines, the reader should see C. DeBoor, J. Approx. Theory 6, 50 (1972).

[25]I. D. Reid, Aust. J. Phys. 32, 231 (1979). Reid has kindly provided us with a copy of his Monte Carlo computer code which was used to perform the calculations included in Table I at 12×10^{-17} V cm^2. The reference cited gives values quoted in Table I at 1×10^{-17} and 24×10^{-17} V cm^2.